Analysis Fast of Neutron Flux and Collision Density Using a Computer Program FASTFLUX

Lee Yoon-joon

FASTFLUX를 이용한 고속중성자의 에너지 분포 해석

李 潤 俊

Summary

The energetic neutrons emitting with fission slow down to become thermal neutrons by losing their energies through the collisions with moderator nuclei. This slowing down process is analyzed by breaking down the fast energy range into several sub-energy groups(multi-group) and once the energy dependent cross sections are known, the neutron flux and neutron collision density in each sub-energy group can be found. For this, a computer program FASTFLUX is established and following topics are discussed in this paper.

1) comparison of analytical values of neutron flux and collision density with the values of FASTFLUX
2) effects of neutron source function on flux
3) effects of moderator mass on discontinuities of collision density
4) effects of resonance absorber and moderator mass on flux

1. Introduction (Theory of FASTFLUX)

Over the energy range of about 2 Mev with which fast neutrons emit to about 1 ev, the neutron energy is so much larger than kT that it may be assumed that there is no upscattering. However, as seen from the relation of that scattering angle μ_0 is eaual to $0.07A^{-1}E$, the anisotropic elastic scattering measured in COM system tends to be larger with the increase of neutron energy and of moderator mass. For an instance, the anisotropic scattering becomes significant when the neutron energy is above approximately 1 Mev, whereas for a heavier element such as oxygen the p-wave scattering(anisotropic scattering)

理工大學 專任講師

becomes dominant when the energy is above about 50 Kev. But actually the neutron moderation is governed by light material such as hydrogen or oxygen, and this fact permits the assumption that overall scattering can be treated as s-wave scattering.

Accordingly, under three assumptions of: 1) no upscattering, 2) s-wave scattering(Lamarsh, J. R., 1966) and 3) spatially independent, the neutron slowing down equation can be written as;

$$\int_E \Sigma_t(E)\,\phi(E)\,dE = \int dE \int_{E'=E}^{E_{max}} \Sigma_s(E'\rightarrow E)\,\phi(E')\cdot dE' + \int S(E)\,dE \quad \cdots\cdots (1)$$

Where $\Sigma_t(E)$=total macroscopic cross section at energy E, cm^{-1}

$\phi(E)$=neutron flux per unit energy

E_{max}=maximum energy of fast region

S(E)=source density per unit energy

$\Sigma_s(E'\rightarrow E)$=scattering cross section from E′ to E, cm^{-1}

The above equation is self-explanatory based on the conception of continuity in the energy interval of dE about E. By breaking down the entire energy group into G groups, following equation can be obtained.

$$\int_{E_g}^{E_{g-1}} \Sigma_t(E)\,\phi(E)\,dE = \int_{E_g}^{E_{g-1}} dE \int_{E_g}^{E_{max}} \Sigma_s(E'\rightarrow E)\cdot \phi(E')\,dE' + \int_{E_g}^{E_{g-1}} S(E)\,dE \quad \cdots\cdots (2)$$

where E_g and E_{g-1} indicate the lower and upper energy of g-th group. Eq. (2) can be expanded as:

$$\int_{E_s}^{E_{g-1}} \Sigma_t(E)\,\phi(E)\,dE = \int_{E_g}^{E_{g-1}} dE \left[\int_{E_g}^{E_{g-1}} \Sigma_s(E'\rightarrow E)\cdot \phi(E')\,dE' + \int_{E_{g-1}}^{E_{g-2}} \Sigma_s(E'\rightarrow E)\,\phi(E')\,dE' \cdots\cdots + \int_{E_1}^{E_{max}} \Sigma_s(E'\rightarrow E)\,\phi(E')\,dE'\right] + \int_{E_g}^{E_{g-1}} S(E)\,dE \quad \cdots\cdots (3)$$

If the energy interval of a given group is fine, each term of above equation is appoximated as below.

$$\int_{E_g}^{E_{g-1}} \Sigma_t(E)\,\phi(E)\,dE = \Sigma_{tg}\,\phi_g, \int_{E_g}^{E_{g-1}} dE \int_{E_{g'}}^{E_{g'-1}} \Sigma_s(E'\rightarrow E)\cdot \phi(E')\,dE' = \Sigma_{g'g}\phi_{g'}\,,\ \int_{E_g}^{E_{g-1}} S(E)\,dE = S_g \quad \cdots\cdots (4)$$

By plugging these expressions into Eq. (3), the following equations (5) and (6), which are basic underlying equations of FASTFLUX, are obtained.

$$\Sigma_{tg}\phi_g = \sum_{g'=1}^{g} \Sigma_{g'g}\phi_{g'} + S_g \quad \cdots\cdots (5)$$

$$\phi_g = \frac{1}{\Sigma_{tg}-\Sigma_{gg}}\left[\sum_{g'=1}^{g} \Sigma_{g'g}\phi_{g'} + S_g\right],$$

$$g = 1, 2, \cdots\cdots G \quad \cdots\cdots (6)$$

where Σ_{gg} is the self scattering cross section.

2. Numerical procedures of FASTFLUX

From Eq. (6), the flux of each group is in the form of:

$$\phi_1 = \frac{1}{\Sigma_{t1}-\Sigma_{11}}(S_1),\ \phi_2 = \frac{1}{\Sigma_{t2}-\Sigma_{22}}(\Sigma_{12}\phi_1 + S_2),\ \phi_3 = \frac{1}{\Sigma_{t3}-\Sigma_{33}}(\Sigma_{13}\phi_1 + \Sigma_{23}\phi_2 + S_3),$$

and these are calculated easily by FASTFLUX, if group constants are known. At first, Σ_{tg} is defined as $\frac{\int_g \Sigma_t(E)\phi(E)dE}{\int_g \phi(E)dE}=\Sigma_t(\bar{E}_g)$, where $\bar{E}_g$ is the average energy of g-th group, that is, $\bar{E}_g=(E_g+E_{g-1})/2$. If several elements are present, the macroscopic total cross section is simply as follows.

$$\Sigma_t(\bar{E}_g)=\sum_j N_j\,\sigma^j{}_{tg}(\bar{E}_g) \quad \cdots\cdots (7)$$

where N_j=atom(nucleus) density of j-th element, atoms/barn · cm

$\sigma^j{}_{tg}(\bar{E}_g)$=microscopic total cross section of j-th element, g-th energy group evaluated at E, cm^{-2} sec^{-1}.

As in the same way, the group cross section is:

$$\Sigma_{g'g}=\sum_j N_j\,\sigma^j_{g'g}(\bar{E}_g) \quad \cdots\cdots (8)$$

By the assumption of isotropic elastic scattering,

$$\sigma^j_{g'g}=\left(\int_{g'}\int_g \frac{4\pi\,\sigma^j_{cm}(E',\theta_c)}{(1-\alpha_j)E'}\cdot\phi(E')dE'dE\right)$$

$$\left(\int_{g'}\phi(E')dE'\right) \quad \cdots\cdots (9)$$

where $\alpha_j=\left(\frac{A_j-1}{A_j+1}\right)^2$, A_j=atomic mass of j-th element

$\sigma^j{}_{CM}$=elastic scattering cross section of j-th element

But since θ_c is given as $\cos\theta_c=\frac{E'}{(1-\alpha_j)}\left[\frac{2E}{E'}-(1+\alpha_j)\right]$, if $E<\alpha_j E'$, then $\cos\theta_c$ becomes smaller than -1, which says that the self scatering cross section can have its value only when $E\geqq\alpha_j E'$. Since again, when isotropic, $\sigma_{jCM}(E',\theta_c)=\frac{\sigma^j{}_{sg'}}{4\pi}$, $\phi(E')$~constant in g'-th group and $\sigma^j{}_s(E')=\sigma^j{}_{sg'}=\sigma^j{}_{sg'}(\bar{E}_{g'})$~constant in g'-th group, Eq. (9) has the form of,

$$\phi^j_{g'g}=\frac{\sigma^j_{sg'}}{\Delta\bar{E}_{g'}(1-\alpha_j)}\int_{g'}\int_g \frac{dE'}{E'}\cdot dE\cdot$$

$$H(E-\alpha_j E') \quad \cdots\cdots (10)$$

where $H(x)=0,\ x<0$

$=1,\ x\geq 0$

With regard to the source, two options are available in FASTFLUX. The first option is such that the source is of the normalized monoenergetic source, that is, $S_g=S_1=1.0$, otherwize zero. As the second option the normalized distributed source of $S(E)=\chi(E)=\text{constant}\cdot\int_{E_C}^{E_{max}}\exp(-E)\cdot\sinh\sqrt{2E}\cdot dE$ is used with the condition of E(cut-off) $=10^4$ev. If neutron energy is less than 10^4 ev, it is assumed that there is no source. The constant of above source equation is determined automatically in FASTFLUX in such a manner of making the integral, from cut-off energy to E_{max}, unity.

As an additional alternative, geometrical buckling can be takent into account in FASTFLUX. In this case, the flux is calculated by following eguation which is similar to Eq. (6) except the denominator.

$$\phi_g=\frac{1}{\Sigma_{tg}-\Sigma_{gg}-D_g B^2}\left[\sum_{g'=1}^{g-1}\Sigma_{g'g}\phi_{g'}+S_g\right]$$

$$\cdots\cdots (11)$$

where $D=\frac{1}{3\left(\Sigma_{tg}-\sum_j (2N_j\sigma^j_{gs})/(3A_j)\right)}$

On the basis of the assumptions and eguations discussed above is established FASTFLUX, of which the schematic structure is shown is Figure 1, and several small size slave subroutines are included in each major subroutine. The features of the Program are such that it can treat as many

energy groups and elements as the core size permits. For a typical running for water with 300 groups, it takes about 10 minutes on Z-80 series CPM system machine.

3. Results of FASTFLUX

A. Analytical values of flux and collision density vs. FASTFLUX values

For three kinds of hydrogen(A=1), oxygen(A=16) and water, FASTFLUX is run using actual cross section data(BNL-325 2nd ed.), whose results are summarized and compared with analytical values in Table 1 thru 3. As input conditions, the entire energy range of 1.0 Mev to 1.0 ev is divided into 300 groups for all cases. Further, monoenergetic source is used and buckling is not considered.

When A=1, theory says that, with the assumption of no absorption, flux and collision density are given by;

$$\phi(E)=\frac{S}{E\Sigma_s(E)}, \text{ and } F(u)=S=1.0=\text{constant} \quad \cdots\cdots (12)$$

On the other hand, FASTFLUX calculates $\phi(E)$ in accordance with Eq. (6) and F(u) with;

$$F(u)=\frac{-F(E)dE}{du}=\frac{\Sigma_s(E)\phi(E)}{E}\left(\sim\frac{\Sigma_{tg}}{\Sigma_{tg}-\Sigma_{gg}}\right) \quad \cdots\cdots (13)$$

Comparing above two eguations, the anlytical one shows that $\phi(E)$ or F(u) is independent of the cross section(no absorption), while FASTFLUX values depend on group constants. As shown in Table 1, $\Sigma_t=\Sigma_s$ over the range of 1.0 Mev to 1500 Kev in FASTFLUX, and its values of flux/ev and collision density/lethargy are exactly same as anlytical values. When the energy is lower than ~1500 Kev, Σ_t is larger than Σ_s, which means the presence of absorption contrary to the assumption of Eq. (12), and FASTFLUX values are somewhat smaller than those of Eq. (12).

For a case of A>1 (oxygen), with no absorption, the analytical solutions of collision density are (Duderstadt, J. J., 1976):

$$F_0(u)=SH\cdot\exp(H\alpha u),\quad \alpha E_0<E<E_0$$

$$F_1(u)=SH(1-\alpha^H)\exp(H\alpha u)-SH^2\alpha^{H\alpha}(u-\ln\frac{1}{\alpha})\exp(H\alpha u),\quad \alpha^2E_0<E<\alpha E_0$$

$$\vdots$$

$$F_n(u)=F_n(n\ln(\frac{1}{\alpha}))\exp[\alpha H(u-n\ln(\frac{1}{\alpha}))]-\frac{1}{1-\alpha}\int_{\alpha}^{u}du'\cdot F_{n-1}(u'-\ln(\frac{1}{\alpha}))\exp[H\alpha(u-u')],\quad \alpha^{n+1}E_0<E<\alpha^nE_0 \quad \cdots\cdots (14)$$

where $H=\frac{1}{1-\alpha}$, $\alpha=n\ln(1/\alpha)$

If $E<\alpha^3E$, that is in asymptotic regin,

$$F(u)=S/\xi \quad \cdots\cdots (15)$$

Then once F(u) being known,

$$\phi(E)=F(u)/E\Sigma_s(E) \quad \cdots\cdots (16)$$

Table 2 shows the results of FASTFLUX and analytical values obtained by the use of equations (14) thru (16). As can be found in Table 2, big errors occur around the energy of $\sim\alpha E$ and $\sim\alpha^2E$, which are due to collision density discontinuites. Taking into account that Σ_t and Σ_s of oxygen are equal each other thru all energies, then the errors in higher energy groups are due to the value of group average energy, $\bar{E}_g$. In FASTFLUX the energy is broken down into multigroup with equal delta lethargy and the energy band of the higher energy group is larger than that of lower energy group, which, in turn, results in bigger errors.

For the compounded moderator, e. g., water, the analytical solutions are very complicated but in asymptotic region they are(Henry A. G., 1975):

$$F(E) = S / \bar{\xi}(E)E,$$

$$\phi(E) = S / \bar{\xi}(E)\Sigma_s(E) \quad \cdots\cdots (17)$$

where $\bar{\xi}(E) = \frac{1}{\Sigma_s(E)} \Sigma \bar{\xi}_i \Sigma_s^i(E)$

$$= \frac{1}{\Sigma_s(E), \text{water}} [\xi_H \Sigma_S^H(E) + \xi_O \Sigma_s^O(E)]$$

In Table 3. analytical values are calculated for the asymptotic region only. and are compared with FASTFLUX. Table 3 reads that when energy is below $\sim(0.7785)^{\wedge}3 * E_{max} = 0.472\ E+6$ (17th group). both are exactly same.

B. Monoenergetic source vs. distributed source

FASTFLUX is used to check the effect of source functin on the collision density of each group. The collision density per unit lethargy is calculated first with a monoenergetic source and then with a distributed source for hydrogen. oxygen and water respectively. Figure 2. 3. and 4 show the results of each case. In runing the Program. real cross section data are used and other input conditions are same as Section 3-A. except source conditions. For the hydrogen of distributed source. $\phi(E) = \frac{1}{E\Sigma_s(E)} \int_{E_0}^{E_1} S(E')dE'$ in analytical form and FASTFLUX takes E_0 as 1.0 Mev. E_1 as 10^4 ev and $S(E)$ as $\chi(E)$.

Figure 2 shows that with distributed source. the shape of collision density. F(u). is exactly same as the soure functin itself down to the cut-off point(10^4ev). and below the cut-off. F(u) is 1.000. same as the case of monoenergetic source. For the monoenegetic source. the collision density looks like a delta function of $\delta(E_0)$, where E_0 is the average energy of the first group. This is reasonable since both sources are normalized. the area under each curve should be same.

The results of oxygen are shown in Figure 3. In case of the monoenergetic source. discontinuities are observed in high energies. but F(u) smoothly approaches to the maximum value of 8.351. This is because the distributed source can be regarded as the superposition of discrete sources of different energies. therefore discontinuities generated by each discrete source cancel themselves each other. And the limited scattering distance(limited bullet distance. αE) of the oxygen results in the monoincrease of F(u) with the increase of lethargy. In connection with this. it may be noted that the energy point at which the maximum rate of increase occurs coincides with the point where the source intensity is maximum. Further Figure 3 indicates that when the energy is below $\sim \alpha E$(cut-off). two cases of source condition are almost equal. but this is a particular situation of oxygen since α of oxygen is comparatively small(i.e., the distance from the cut-off energy is long). and for heavier element whose α is large. two cases will be identical only in asymptotic region of below $\alpha^2 E$(cut-off).

For water(Figure 4). discontinuities are found at $E = \alpha_1 E_{max}$ and $\alpha_0^2 E_{max}$ by the effect of oxygen. However below the energy of $\alpha_0^2 E_{max}$. both cases show similar pattern. And F(u) of distributed source is somewhat larger then that of monoenergetic source because the spread of source effects the lower energy groups.

C. Effects of mass on discontinuities of collision density

For the evaluation of the effect of mass on discontinuities of F(u). five cases of A=2. 4. 12. 16. and 150 are tested and Figure 5 is obtained. One hundred groups are used over 1.0 Mev to 1.0 ev and to eliminate the effect of cross sections

whatsoever, fictitious cross section data(hydrogen) are used for all cases. In Figure 5, the variable $(1-\alpha)$ F(u) is plotted in terms of $u/\ln(\frac{1}{\alpha})$. Discontinuities are shown at $u/\ln\frac{1}{\alpha}=1.2\cdots(E=\alpha E_0, \alpha^2E_0\cdots)$, and the magnitude of discontinuity at $u/\ln(\frac{1}{\alpha})=1$ becomes significant with the increase of mass. Particularly in the asymptotic region, $(1-\alpha)F(u)$ converges to 2.0 as expected since $(1-\alpha)F(u)=[4A/(A+1)]\times[(A+2/3)/2]=2.0$ if A is sufficiently large.

D. Effects of resonance absorber and mass on neutron flux

To evaluate the resonance absorption, energy range is assumed to be from 1000.0 ev to 950.0 ev and 300 groups are used. As for a resonance absorber, uranium-238 of 2471 barns at 966.6 ev and 966.5 ev (group No. 199 and 200) are assumed. By using the real cross section data, EASTFLUX is run for A=1, 16 and water whose results are briefed in Table 4. In addtion with fictitious cross secsions(hydrogen), same procedures are taken for A=50, and 150, and Table 5 shows the results of these cases.

As expected, since no upscattering is permitted, the fluxes in all the higher energy groups than the resonance group(No. 199) are same for both cases of "dirty" and "clean". The flux drops not only in resonance groups but also in all lower energy groups. For hydrogen, the magnitude of deviation between dirty and clean is almost constant thru all lower energy groups. But this deviation becomes more significant with the increase of mass and with the decrease of energy. This is because the larger the α (the larger the mass), the larger the probability of falling into resonance pitfalls. And once being caught in pitfalls, that portion of neutron flux can not play its role of the source with respect to lower energy groups, therefore with the increase of lethargy, this effect accumulates.

Of interest is the case when black absorber of $\sigma_a=10^{10}$ barns is assumed to present in 199th and 200th groups. The results are almost same as the case of 2471 barns. This means that if $\Sigma_a \gg \Sigma_s$, the fluxes in lower energy groups do not depend on the absolute value of Σ_a but rather on width Γ. If Doppler broadening occurs, the fluxes will show different values because of the wider Γ.

The last column in Table 5 shows this broadening effect. Without being changed the total quantity of 741 barns (cf. 2471 barns/ev x 0.3ev) in 199th and 200th groups, σ_a is distributed over five groups, from 198th thru 202nd group. The results show that the values of dirty case are lower than clean case by about 3 per cent.

Finally, if $\Gamma(\Delta E)\ll E_{reso}$, and $E_{reso}\ll\alpha^3E_0$, as the case of A=150 in Table 5, then the resonance escape probability can be obtained easily as follows.

By letting the upper and lower boundary energy of the resonance group be E_a, E_b, respectively and $\Delta E=E_a-E_b$, then $F(E)=S/\xi E$ in asymptotic region. The total number of neutrons crossing E_b is, when black absorber,

$$q=\int_{E_a}^{E_b/\alpha}F(E')dE'\frac{E_b-\alpha E'}{(1-\alpha)E'}$$

$$=\frac{S}{(1-\alpha)\xi}\int_{E_a}^{E_b/\alpha}\frac{(E_b-\alpha E')}{E'^2}\cdot dE'$$

$$=\frac{1}{(1-\alpha)\xi}\left[\frac{E_b}{E_a}-\alpha-\alpha\ln\frac{E_b}{\alpha E_a}\right]$$

Since $E_a=E_{reso}+\frac{\Delta E}{2}$, $E_b=E_{reso}-\frac{\Delta E}{2}$, $E_b/E_a=1-\Delta E/(E_{reso}+\Delta E/2)=1-\Delta E/E_{reso}$ then

the escape probability $=p=1-\frac{1}{(1-\alpha)\xi}$.

$$[\frac{\triangle E}{E_{reso}}+\alpha \ln (1-\frac{\triangle E}{E_{reso}})]=1-\frac{\triangle E}{\xi E_{reso}}$$

The resonace escape probability of A=150 in Table 5. calculated by above equation, is

$p=1-0.3/(0.0133\times 960)=0.977$.

4. Conclusion

FASTFLUX is comprised of relatively simple algorithms, but as dicussed in above, it renders satisafactory results. Particularly in the vicinity of source energy in which analytical solution are cumbersome to obtain, or when absorption is present, it can be used without any limitation as far as cross section data are available. The major limitation of the Program is that it excludes the spatial dependence of flux. When a reactor is finite and/or heterogeneous, as usually is, the flux should be described by the function of position as well as of energy. For this, group constants should be determined at every position and energy of interest, which could be obtained by group collapse procedure. However, aside from the position vector, FASTFLUX could be used to estimate the overall characteristics of fast fluxes at the preliminary stage of design or easily be modified to become a subroutine in calculating spatially dependent fluxes.

Group No.	Group Avg Energy, ev	Σt cm^{-1}	Σs cm^{-1}	Flux/ev		Collision Density		Remark
				Analytical	FASTFLUX	Analytical	FASTFLUX	
1	0.9775E+06	0.2887	0.2887	0.3544E-05	0.7877E-04	0.1000E+01	0.2223E+02	SOURCE
2	0.9335E+06	0.2975	0.2975	0.3601E-05	0.3602E-05	0.1000E+01	0.1000E+01	
10	0.6458E+06	0.3668	0.3668	0.4222E-05	0.4223E-05	0.1000E+01	0.1000E+01	
30	0.2571E+06	0.5999	0.5999	0.6484E-05	0.6486E-05	0.1000E+01	0.1000E+01	
50	0.1024E+06	0.8481	0.8481	0.1151E-04	0.1152E-04	0.1000E+01	0.1000E+01	
70	0.4075E+05	1.0930	1.0930	0.2245E-04	0.2246E-04	0.1000E+01	0.1000E+01	
100	0.1024E+05	1.2820	1.2820	0.7617E-04	0.7624E-04	0.1000E+01	0.1000E+01	
120	0.4075E+04	1.3190	1.3190	0.1860E-03	0.1862E-03	0.1000E+01	0.1000E+01	
140	0.1622E+04	1.3340	1.3340	0.4622E-03	0.4624E-03	0.1000E+01	0.1000E+01	
181	0.2455E+03	1.3580	1.3570	0.3002E-02	0.2999E-02	0.1000E+01	0.1000E+01	
193	0.1413E+03	1.3610	1.3600	0.5203E-02	0.5199E-02	0.1000E+01	0.9997E+00	
222	0.3716E+02	1.3630	1.3610	0.1977E-01	0.1972E-01	0.1000E+01	0.9988E+00	
241	0.1549E+02	1.3630	1.3610	0.4743E-01	0.4728E-01	0.1000E+01	0.9980E+00	
281	0.2455E+01	1.3640	1.3610	0.2922E+00	0.2971E+00	0.1000E+01	0.9952E+00	
287	0.1863E+01	1.3650	1.3610	0.3944E+00	0.3913E+00	0.1000E+01	0.9945E+00	
292	0.1479E+01	1.3650	1.3610	0.4968E+00	0.4923E+00	0.1000E+01	0.9940E+00	
300	0.1024E+01	1.3650	1.3610	0.7175E+00	0.7109E+00	0.1000E+01	0.9930E+00	

Table 1. Flux and Collision densily vs. energy group — hydrogen

Group No.	Group Avg Energy,ev	Group Lethargy	Σt_1 cm^{-1}	Σs_1 cm^{-1}	Flux/ev		Collision Density		Remark
					Analytical	FASTFLUX	Analytical	FASTFLUX	
1	0.9775E+06	0.2276E-01	0.1657	0.1657	0.3020E-04	0.1496E-03	0.4892E+01	0.2422E+02	Source Group
2	0.9335E+06	0.6881E-01	0.1481	0.1481	0.4160E-04	0.3879E-04	0.5751E+01	0.5363E+01	
3	0.8915E+06	0.1149E+00	0.1313	0.1313	0.5777E-04	0.5389E-04	0.6763E+01	0.6309E+01	~7% error
4	0.8514E+06	0.1609E+00	0.1153	0.1153	0.8098E-04	0.7560E-04	0.7950E+01	0.7422E+01	~7% error
5	0.8130E+06	0.2070E+00	0.1000	0.1000	0.1150E-03	0.1074E-03	0.9349E+01	0.8731E+01	~7% error
6	0.7765E+06	0.2530E+00	0.0980	0.0980	0.1445E-03	0.1258E-03	0.1099E+02	0.9572E+01	~11% error, ~alpha*Emax
7	0.7415E+06	0.2991E+00	0.1026	0.1026	0.9853E-04	0.1041E-03	0.7496E+01	0.7926E+01	~5% error
8	0.7081E+06	0.3451E+00	0.1071	0.1071	0.1000E-03	0.1061E-03	0.7590E+01	0.8045E+01	~6% error
9	0.6763E+06	0.3912E+00	0.1114	0.1114	0.9800E-04	0.1106E-03	0.7383E+01	0.8334E+01	~12% error
10	0.6458E+06	0.4372E+00	0.1155	0.1155	0.9209E-04	0.1137E-03	0.6869E+01	0.8476E+01	~23% error
11	0.6168E+06	0.4833E+00	0.1194	0.1194	0.8074E-04	0.1145E-03	0.5946E+01	0.8428E+01	~41% error, ~alpha^2*Emax
17	0.4679E+06	0.7596E+00	0.1881	0.1881	0.9473E-04	0.9481E-04	0.8337E+01	0.8343E+01	~0.1% error, <alpha^3*Emax
22	0.3716E+06	0.9898E+00	0.1742	0.1742	0.1288E-03	0.1290E-03	0.8337E+01	0.8350E+01	~0.1% error
50	0.1024E+06	0.2279E+01	0.1237	0.1237	0.6582E-03	0.6597E-03	0.8337E+01	0.8352E+01	~0.17% error
100	0.1024E+05	0.4582E+01	0.1237	0.1237	0.6582E-02	0.6597E-02	0.8337E+01	0.8352E+01	~0.17% error
150	0.1024E+04	0.6884E+01	0.1237	0.1237	0.6582E-01	0.6596E-01	0.8337E+01	0.8351E+01	~0.16% error
200	0.1024E+03	0.9187E+01	0.1237	0.1237	0.6582E+00	0.6594E+00	0.8337E+01	0.8349E+01	~0.14% error
250	0.1024E+02	0.1149E+02	0.1237	0.1237	0.6582E+01	0.6593E+01	0.8337E+01	0.8347E+01	~0.12% error
300	0.1024E+01	0.1379E+02	0.1237	0.1237	0.6582E+02	0.6588E+02	0.8337E+01	0.8341E+01	-0.05% error

Table 2. Flux and Collision density vs. energy group — oxygen

Group No.	Group Avg Energy,ev	$\bar{\xi}(H_2O)$	Flux/ev		Collision Density		Remark
			Analytical	FASTFLUX	Analytical	FASTFLUX	
1	0.9775E+06	0.6792E+00	---	0.5159E-04	---	0.2291E+92	Source Group
2	0.9335E+06	0.7075E+00	---	0.5816E-05	---	0.2419E+01	
3	0.8915E+06	0.7357E+00	---	0.6532E-05	---	0.2546E+01	
17	0.4679E+06	0.7348E+00	0.4661E-05	0.4554E-05	0.1361E+01	0.1330E+01	~2.3% error,<alpha^3*Emax
22	0.3716E+06	0.7727E+00	0.5162E-05	0.5346E-05	0.1294E+01	0.1340E+01	~3% error
50	0.1024E+06	0.8880E+00	0.1132E-04	0.1137E-04	0.1126E+01	0.1131E+01	~0.4% error
100	0.1024E+05	0.9224E+00	0.7529E-04	0.7542E-04	0.1084E+01	0.1085E+01	exactly same
150	0.1024E+04	0.9253E+00	0.7226E-03	0.7230E-03	0.1081E+01	0.1081E+03	exactly same
200	0.1024E+03	0.9265E+00	0.7091E-02	0.7093E-02	0.1079E+01	0.1079E+01	exactly same
250	0.1024E+02	0.9272E+00	0.7084E-01	0.7076E-01	0.1078E+01	0.1076E+01	exactly same
300	0.1024E+01	0.9273E+00	0.7075E+00	0.7033E+00	0.1078E+01	0.1071E+01	~0.6% error

Table 3. Flux and Collision density vs. energy group — water

Group No.	Group Avg Energy,ev	Hydrogen		Oxygen		Water		Remark
		Clean	Dirty	Clean	Dirty	Clean	Dirty	
1	0.9999E+03	0.4375E+01	0.4375E+01	0.4730E+02	0.4730E+02	0.4004E+01	0.4004E+01	Source Group
2	0.9997E+03	0.7481E-03	0.7481E-03	0.3656E-01	0.3656E-01	0.8887E-03	0.8887E-03	
10	0.9984E+03	0.7488E-03	0.7488E-03	0.3672E-01	0.3672E-01	0.8898E-03	0.8898E-03	
20	0.9967E+03	0.7503E-03	0.7503E-03	0.3705E-01	0.3705E-01	0.8920E-03	0.8920E-03	
30	0.9950E+03	0.7517E-03	0.7517E-03	0.3738E-01	0.3738E-01	0.8943E-03	0.8943E-03	
50	0.9916E+03	0.7541E-03	0.7541E-03	0.3793E-01	0.3793E-01	0.8980E-03	0.8980E-03	
100	0.9831E+03	0.7604E-03	0.7604E-03	0.3940E-01	0.3940E-01	0.9078E-03	0.9078E-03	
120	0.9796E+03	0.7628E-03	0.7628E-03	0.3988E-01	0.3988E-01	0.9115E-03	0.9115E-03	
160	0.9731E+03	0.7681E-03	0.7681E-03	0.4128E-01	0.4128E-01	0.9198E-03	0.9198E-03	
190	0.9581E+03	0.7717E-03	0.7717E-03	0.4217E-01	0.4217E-01	0.9254E-03	0.9254E-03	
198	0.9668E+03	0.7729E-03	0.7729E-03	0.4248E-01	0.4248E-01	0.9273E-03	0.9273E-03	
199	0.9666E+03	0.7732E-03	0.6210E-04	0.4255E-01	0.3406E-03	0.9277E-03	0.8080E-04	Resonance Group
200	0.9665E+03	0.7732E-03	0.6210E-04	0.4254E-01	0.3406E-03	0.9277E-03	0.8080E-04	Resonance Group
201	0.9663E+03	0.7734E-03	0.7732E-03	0.4261E-01	0.4254E-01	0.9281E-03	0.9277E-03	
202	0.9661E+03	0.7734E-03	0.7732E-03	0.4260E-01	0.4254E-01	0.9281E-03	0.9277E-03	
205	0.9656E+03	0.7736E-03	0.7734E-03	0.4266E-01	0.4259E-01	0.9284E-03	0.9280E-03	
210	0.9648E+03	0.7749E-03	0.7747E-03	0.4299E-01	0.4292E-01	0.9305E-03	0.9301E-03	
220	0.9632E+03	0.7758E-03	0.7756E-03	0.4322E-01	0.4316E-01	0.9319E-03	0.9315E-03	
230	0.9615E+03	0.7770E-03	0.7768E-03	0.4353E-01	0.4346E-01	0.9337E-03	0.9334E-03	
240	0.9599E+03	0.7782E-03	0.7780E-03	0.4384E-01	0.4377E-01	0.9356E-03	0.9352E-03	
250	0.9582E+03	0.7797E-03	0.7794E-03	0.4422E-01	0.4415E-01	0.9379E-03	0.9375E-03	
260	0.9566E+03	0.7812E-03	0.7809E-03	0.4461E-01	0.4454E-01	0.9402E-03	0.9399E-03	
270	0.9550E+03	0.7826E-03	0.7824E-03	0.4500E-01	0.4493E-01	0.9426E-03	0.9422E-03	
280	0.9533E+03	0.7835E-03	0.7833E-03	0.4524E-01	0.4517E-01	0.9440E-03	0.9436E-03	
290	0.9517E+03	0.7850E-03	0.7848E-03	0.4563E-01	0.4556E-01	0.9463E-03	0.9459E-03	
300	0.9501E+03	0.7856E-03	0.7854E-03	0.4580E-01	0.4572E-01	0.9473E-03	0.9469E-03	

Table 4. Flux with resonance absorber, A=1, 16 and water

Group No.	Group Avg Energy, ev	A=50		A=150				Remark
		Clean	Dirty	Clean	Dirty	BLK. Absorp.	Doppler	
1	0.9999E+03	0.8756E+01	0.8756E+01	0.8769E+01	0.8769E+01	0.8769E+01	0.8769E+01	Source Group
2	0.9997E+03	0.1953E-01	0.1953E-01	0.5748E-01	0.5748E-01	0.5748E-01	0.5748E-01	
10	0.9984E+03	0.1977E-01	0.1977E-01	0.5959E-01	0.5959E-01	0.5959E-01	0.5959E-01	
20	0.9967E+03	0.2029E-01	0.2029E-01	0.6426E-01	0.6426E-01	0.6426E-01	0.6426E-01	
30	0.9950E+03	0.2082E-01	0.2082E-01	0.6930E-01	0.6930E-01	0.6930E-01	0.6930E-01	
50	0.9916E+03	0.2171E-03	0.2171E-01	0.7839E-01	0.7839E-01	0.7839E-01	0.7839E-01	
100	0.9831E+03	0.2422E-01	0.2422E-01	0.1079E+00	0.1079E+00	0.1079E+00	0.1079E+00	
120	0.9798E+03	0.2525E-01	0.2525E-01	0.1219E+00	0.1219E+00	0.1219E+00	0.1219E+00	
160	0.9731E+03	0.2769E-01	0.2769E-01	0.1118E+00	0.1118E+00	0.1118E+00	0.1118E+00	
190	0.9681E+03	0.2945E-01	0.2945E-01	0.1063E+00	0.1063E+00	0.1063E+00	0.1063E+00	
198	0.9668E+03	0.3007E-01	0.3007E-01	0.1199E+00	0.1199E+00	0.1199E+00	0.2151E-01	Doppler Broadening
199	0.9666E+03	0.3021E-01	0.1262E-02	0.1200E+00	0.4993E-02	0.7981E-11	0.1169E-01	Resonance Group
200	0.9665E+03	0.3020E-01	0.1262E-02	0.1204E+00	0.5016E-02	0.8018E-11	0.8080E-02	Resonance Group
201	0.9663E+03	0.3033E-01	0.3020E-01	0.1204E+00	0.1189E+00	0.1188E+00	0.1160E-01	Doppler Broadening
202	0.9661E+03	0.3032E-01	0.3019E-01	0.1209E+00	0.1194E+00	0.1194E+00	0.2123E-01	Doppler Broadening
205	0.9656E+03	0.3043E-01	0.3030E-01	0.1209E+00	0.1194E+00	0.1194E+00	0.1175E+00	
210	0.9648E+03	0.3112E-01	0.3099E-01	0.1150E+00	0.1133E+00	0.1133E+00	0.1113E+00	
220	0.9632E+03	0.3161E-01	0.3147E-01	0.1329E+00	0.1312E+00	0.1312E+00	0.1291E+00	
230	0.9615E+03	0.3225E-01	0.3212E-01	0.1291E+00	0.1273E+00	0.1273E+00	0.1251E+00	
240	0.9599E+03	0.3291E-01	0.3277E-01	0.1243E+00	0.1224E+00	0.1223E+00	0.1200E+00	
250	0.9582E+03	0.3375E-01	0.3361E-01	0.1335E+00	0.1314E+00	0.1313E+00	0.1288E+00	
260	0.9566E+03	0.3461E-01	0.3446E-01	0.1235E+00	0.1213E+00	0.1212E+00	0.1185E+00	
270	0.9550E+03	0.3548E-01	0.3533E-01	0.1479E+00	0.1455E+00	0.1454E+00	0.1425E+00	
280	0.9533E+03	0.3603E-01	0.3587E-01	0.1398E+00	0.1373E+00	0.1372E+00	0.1342E+00	
290	0.9517E+03	0.3694E-01	0.3678E-01	0.1421E+00	0.1394E+00	0.1393E+00	0.1360E+00	
300	0.9501E+03	0.3732E-01	0.3716E-01	0.1193E+00	0.1172E+00	0.1171E+00	0.1137E+00	

Table 5. Flux with resonance absorber, A=50 and A=150(fictitious)

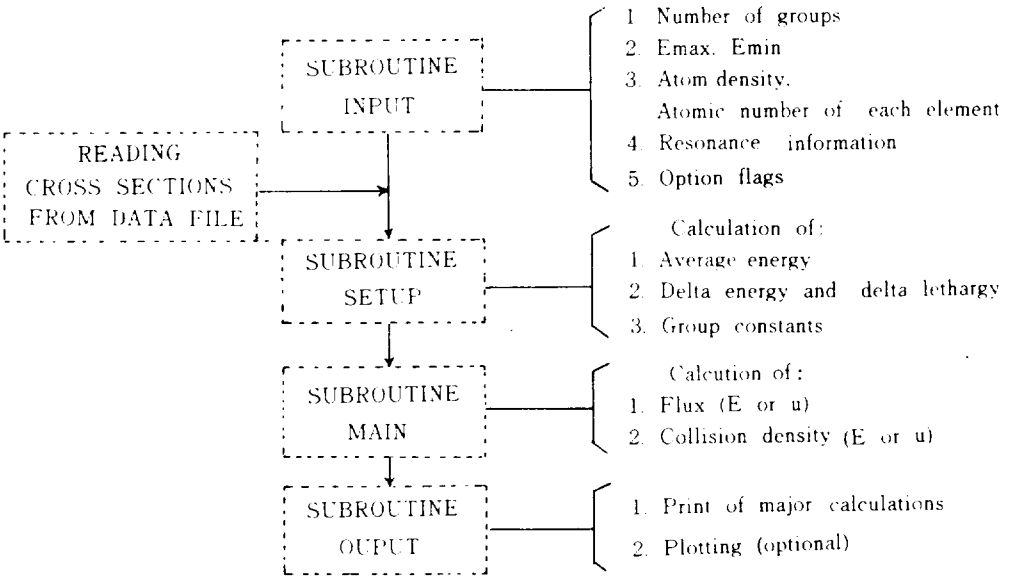

Fig 1. Structure of FASTFLUX

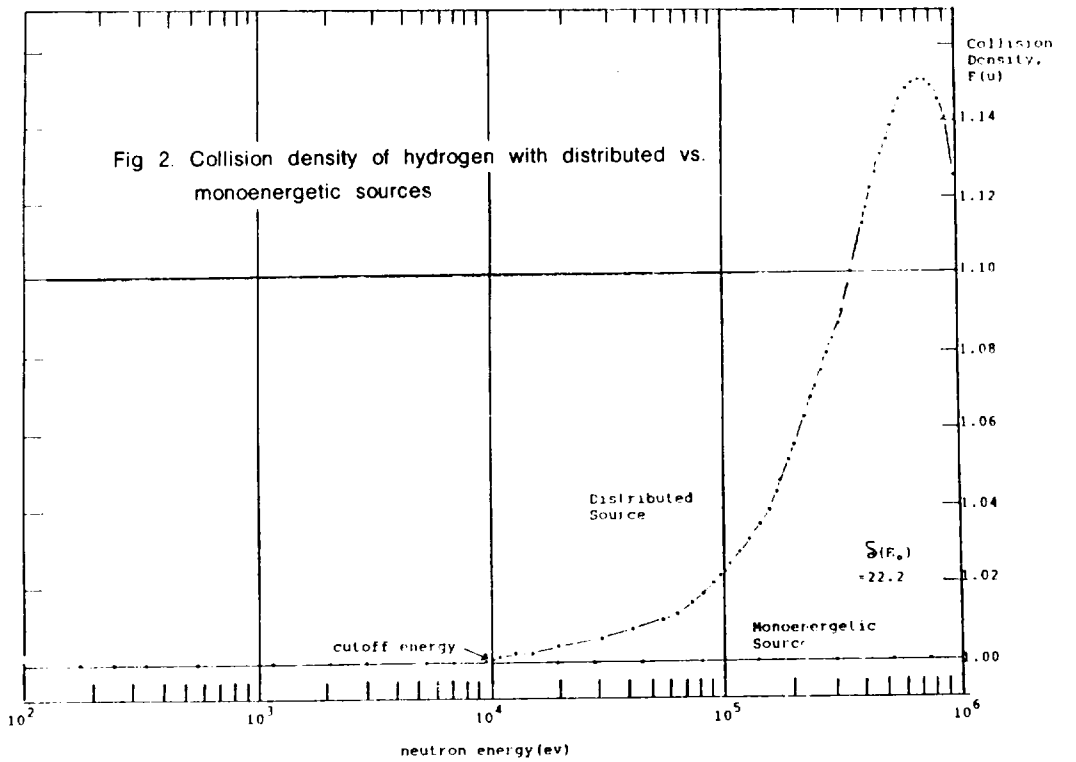

Fig 2. Collision density of hydrogen with distributed vs. monoenergetic sources

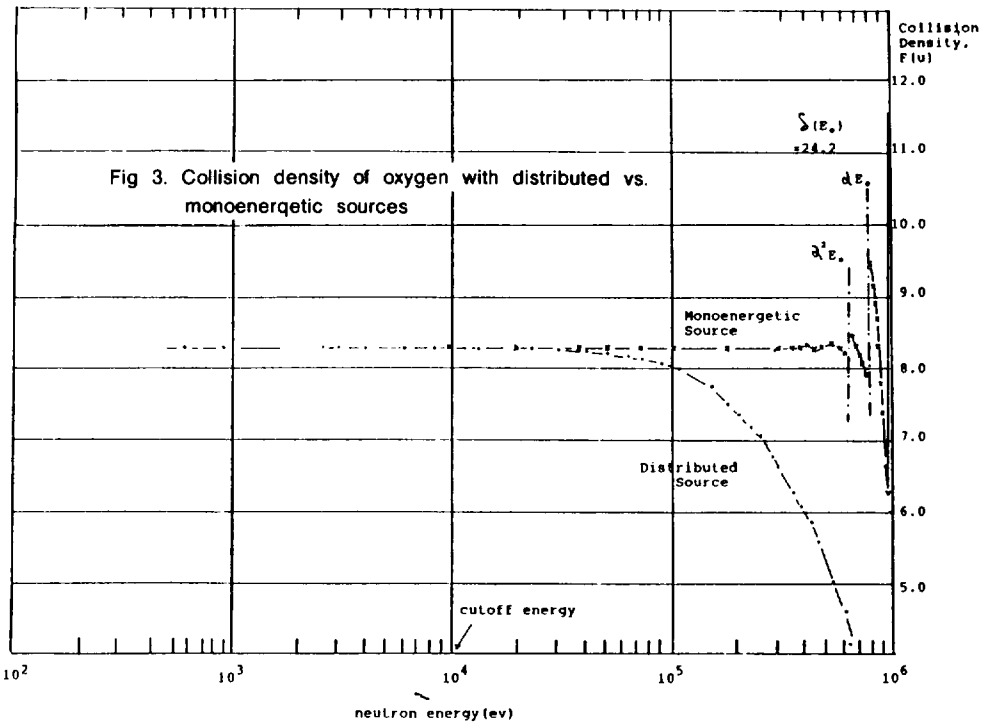

Fig 3. Collision density of oxygen with distributed vs. monoenergetic sources

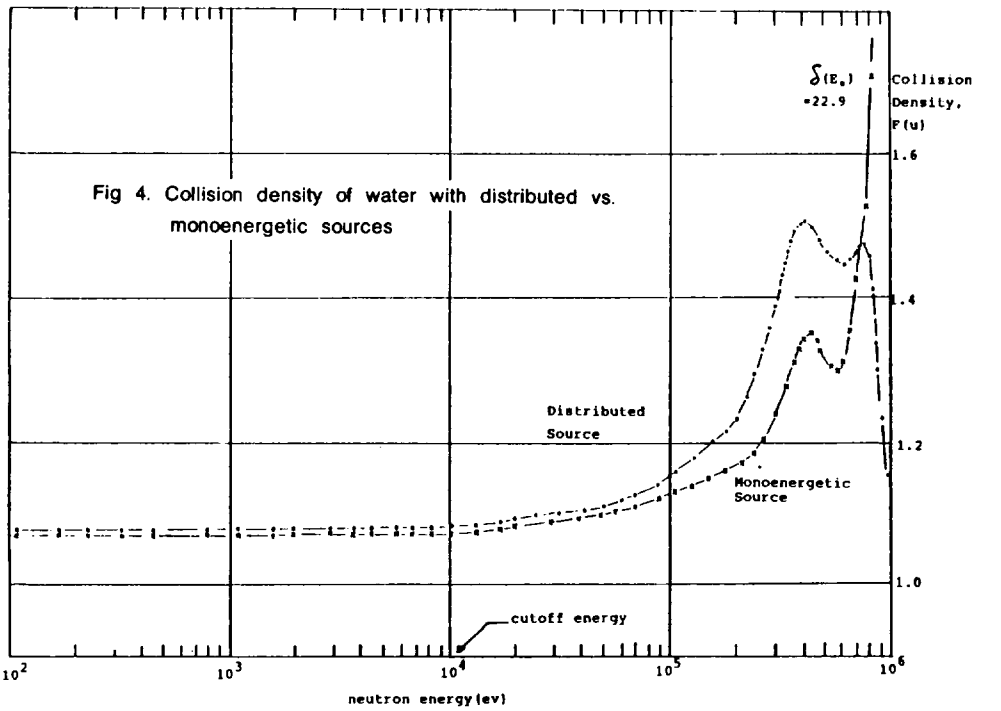

Fig 4. Collision density of water with distributed vs. monoenergetic sources

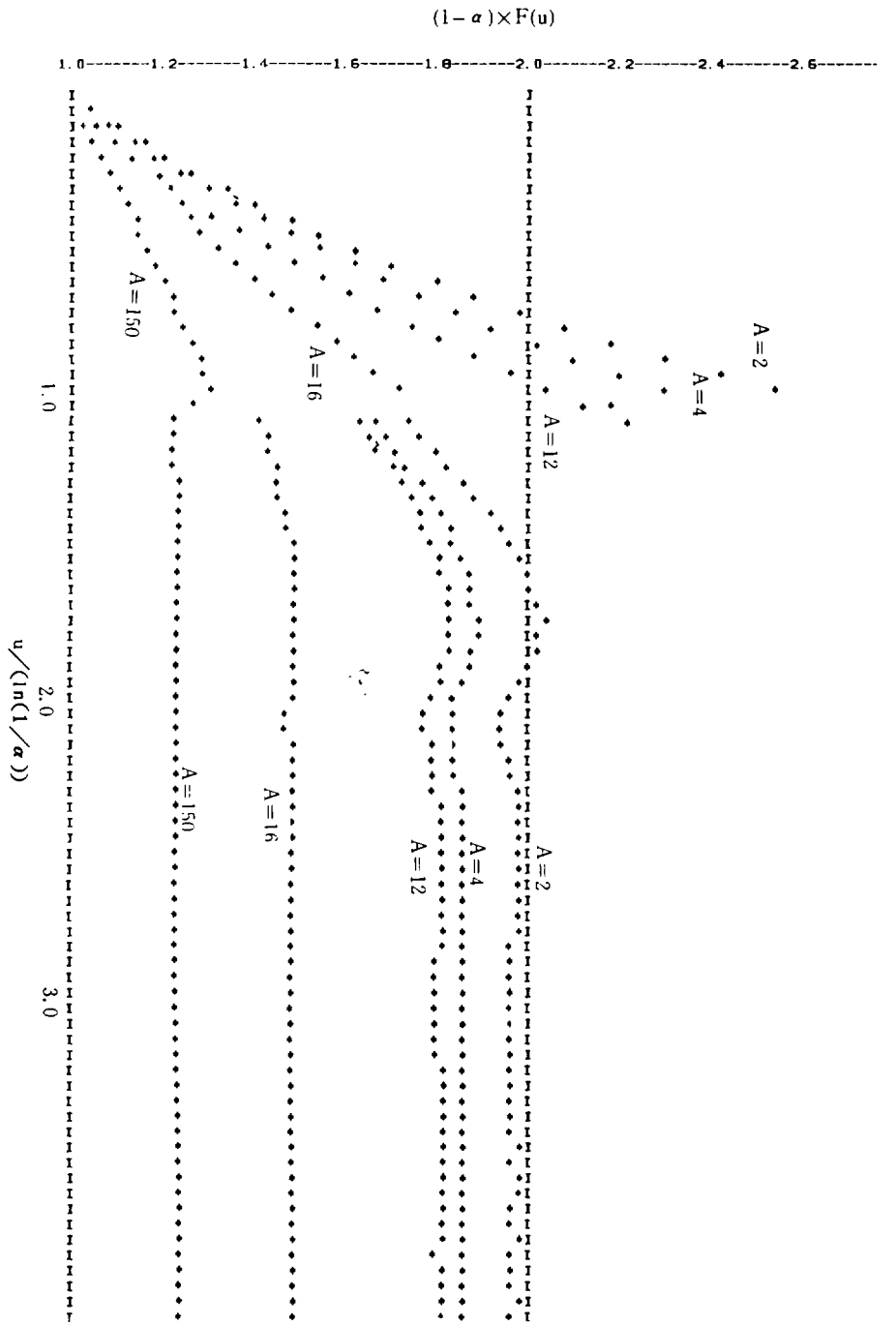

Fig 5. Discontinuities of collision density - Placzek Osallation

Literature Cited

Duderstadt, J. J., et al. 1976. Nuclear Reactor Anaysis, pp. 327–331, John Wiley Sons Inc., U. S. A.

Henry, A. F., 1975. Nuclear Reactor Analysis, the MIT Press, Cambridge, MA. U. S. A.

Hughes, D. J., et al, 1958. Neutron Cross Sections, BNL 2nd ed. pp. 87–90.

Lamarsh, J. R., 1966. Introduction to Nuclear Engineering, pp 39–42. Addison Wesley, MA. U. S. A.

국 문 초 록

핵분열에 의한 중성자가 감속재와의 산란에 의해 고에너지에서 저에너지(열중성자)로 될때의 평형방정식은 수송론에서와 같이 공간, 에너지 및 방향각의 함수가 된다.

본고에서는 무한매질 및 s-wave를 가정하여 중성자 평형식을 에너지만의 함수로 근사시켜 이에 대한 multigroup equation을 FORTRAN으로 작성하였다. 또한 이 프로그램을 이용하여 각 그룹에서의 중성자속을 계산함과 동시 중성자속에 영향을 주는 각종 인자의 성질을 계산하여 multigroulp에 의한 결과와 해석적 방법에 의한 결과를 정량적으로 비교 검토하였다.